AERO 557 Project 1

Steven Sharp

February 20, 2023

Contents

The goal of this project is to predict an overhead pass of a spacecraft visible to the naked eye from the Cal Poly campus by developing a MATLAB program that produces look angles between a ground-based observer and a spacecraft given the spacecraft's TLE, observer's geographic location, and time of observation. Additionally, separately provided observation data was analyzed to determine which of three candidate objects was most likely to have been detected.

1 Optical Observation Prediction

1.1 Prediction and Verification

The Hubble Space Telescope was chosen as the most promising candidate for successful orbit determination and observation on the available evening since its relative brightness was predicted to be as low as 2.4 and its orbit is well known. The TLE used for propagation is as follows:

```
   HST
1  20580U  90037B    23046.55466030   .00008081   00000+0   44819−3  0    9993
2  20580   28.4715  356.6210  0002544  144.8594   19.9327  15.11979697603024
```

The orbital elements at the TLE epoch are:

e	h ($\mathrm{km\,s^{-2}}$)	i (°)	Ω (°)	ω (°)	θ (°)
0.000 254 4	52,475.2	28.7415	356.6210	144.8594	379.9426

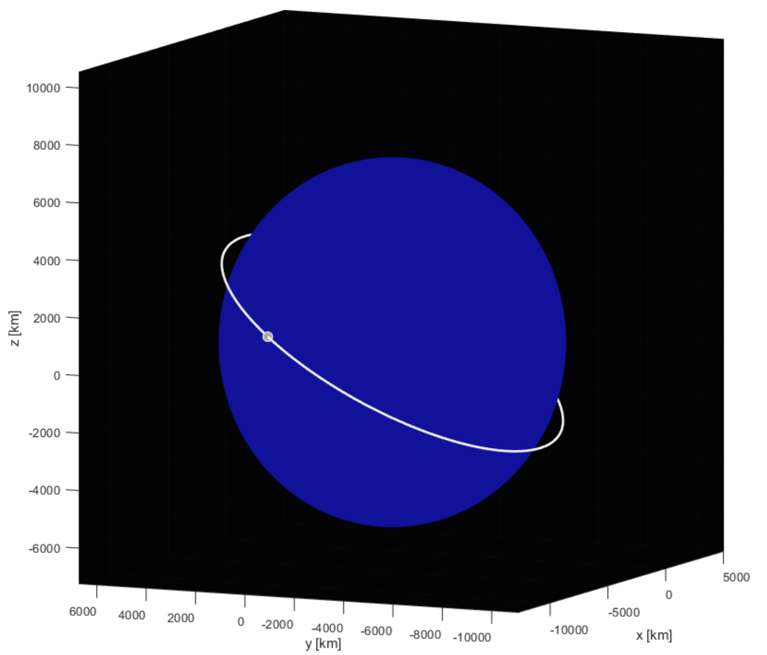

Figure 1 Hubble location at TLE epoch (15 February 2023 13:18:42 UT)

The position of the HST was propagated using `ode45` from the TLE epoch to the visible time predicted by the website *in-the-sky.org* for the coordinates 35° 16.8′ N 120° 39.8′ W. The peak elevation was predicted to occur at 7:12 PM PST, February 15, 2023 (16 February 2023 03:12 UT).

	in-the-sky.org		MATLAB	
Time (UT)	Azimuth	Elevation	Azimuth	Elevation
03:09:09	SW	12°	236.5° (WSW)	8.0°
03:12:24	S	29°	193.6° (SSW)	26.9°
03:13:30	SE	25°	164.5° (SSE)	28.4°
03:14:15			144.81° (SE)	25.0°

The two predictions vary slightly in time but have similar look angles. The MATLAB prediction is 45 seconds behind the website's prediction, but the website was using an older TLE with an epoch of 15 February 04:47:11 UT, which is 8.5 hours before the epoch in the MATLAB program.

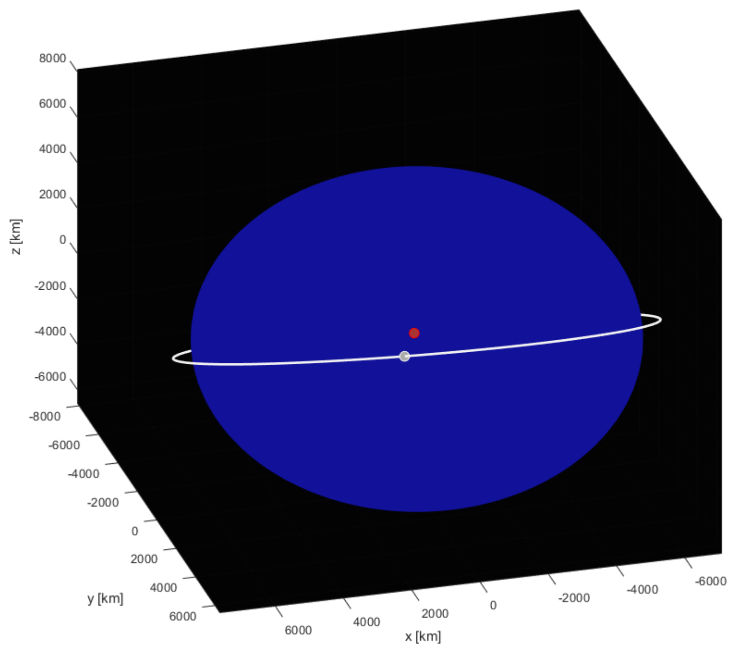

Figure 2 Predicted Hubble and observer location during overhead pass (16 February 2023 03:12:24 UT)

Before heading out to attempt observation, three backup candidates were selected in case of failure to locate the Hubble Space Telescope:

```
SL-16 R/B
1 19120U 88039B   23046.04516806  .00000008  00000+0  26621-4 0  9994
2 19120  71.0136 273.2972 0024241 257.0874 102.7543 14.19289183799644
```

```
CZ-4B R/B
1 29507U 06046C   23046.72889190  .00006032  00000+0  44345-3 0  9991
2 29507  97.7028  80.6307 0045654 130.5889 229.9322 15.02944274891443
```

```
CZ-2C R/B
1 43173U 18011E   23046.35368842  .00051564  00000+0  91753-3 0  9991
2 43173  34.9878   9.1807 0102241 259.4502  99.4687 15.43331037282523
```

The predictions for these three objects were similarly verified with *in-the-sky.org*:

		in-the-sky.org		MATLAB	
	Time (UT)	Azimuth	Elevation	Azimuth	Elevation
SL-16 R/B	03:07:15	ENE	61°	89.0° (E)	45.1°
CZ-4B R/B	03:14:47	NNE	66°	13.4° (NNE)	54.1°
CZ-2C R/B	03:27:42	SSE	70°	178.0° (S)	62.6°

1.2 Observation

The ground station consisting of a spiral-bound notebook, coffee mug, and brass compass was set up at the west end of campus on a dirt path encircling a crop field. Unfortunately, while the location was not blocked by buildings, surrounding trees and artificial lights made it difficult to view celestial objects close to the horizon. As such, the rise and set times were indeterminate but the spacecraft were bright enough to easily discern their location in the sky at peak elevation.

Of the four candidate objects, three were observable, including the Hubble Space Telescope:

	Expected			Observed		
	Time (UT)	Azimuth	Elevation	Time (UT)	Azimuth	Elevation
SL-16 R/B	03:07:15	E/ENE	45-61°	03:08	ENE	~60°
HST	03:13:30	S/SSW	27-29°	03:13	SSW	~25°
CZ-4B R/B	03:14:47	NNE	54-66°	-	-	-
CZ-2C R/B	03:27:42	S/SSE	63-70°	03:26	SE	~80°

The minimal difference in time and look angles between the predictions and observations is surprising, with the Hubble Space Telescope appearing at the correct azimuth and elevation within a minute of the prediction time. For the other two objects, the time was accurate within about two minutes, but the predicted elevation was too low by about 15°. However, given that these two objects are uncontrolled rocket bodies, they were likely subject to more acceleration from perturbations and had a less accurate TLE than the Hubble Space Telescope. All TLEs were also around half a day old when the predictions were made, so the predicted times would have likely been even closer to the correct times if using a freshly published TLE from within the hour.

2 Single and Double Pass Orbit Determination

The following TLEs were given along with a list of observations:

Single Pass

```
   TLE 1
1 25623U 99004C   13109.04882318 -.00000094  00000-0 -16690-3 0  1204
2 25623 051.9974 067.7982 0012092 184.1231 215.4516 11.86494224651645
```

```
   TLE 2
1 25165U 98008D   13083.14572197 -.00000211  00000-0 -12941-2 0  4434
2 25165 052.0160 303.6990 0005433 319.9573 182.6276 12.12023409691559
```

```
   TLE 3
1 25946U 99058D   13104.16396495 -.00000071  00000-0  19175-3 0   939
2 25946 051.9981 329.5396 0000986 149.5293 353.4996 12.46940793622716
```

Double Pass

```
   TLE 4
1 25907U 99049A   13130.15888270 -.00000065  00000-0  26093-3 0   694
2 25907 051.9960 032.8455 0001911 029.4868 130.5755 11.93063529625032
```

```
   TLE 5
1 25852U 99037B   13130.84350436 -.00000077  00000-0  15012-3 0   966
2 25852 052.0023 051.2535 0001668 049.6249 354.2041 12.62268979638190
```

```
   TLE 6
1 25309U 98023D   13130.29943631 -.00000076  00000-0  15976-3 0  1960
2 25309 051.9963 053.4139 0002124 156.5112 343.8142 12.35927962691488
```

To determine which candidate TLE is the best match for the observations, each TLE was converted into the corresponding orbital elements and then propagated back to the time of the middle observation for each pass to determine its true anomaly. Initial orbit determination using the extended Gaussian method was performed on all observations for the single pass and observations 2-4, 5-7 for the double pass, using the middle observation of each set for the results.

2.1 Single Pass

The orbital elements corresponding to the calculated orbit and candidate TLEs for the single pass observation on 25 March 2013 at 3:15:20 UT are as follows:

Object	e	h ($\mathrm{km\,s^{-2}}$)	i (°)	Ω (°)	ω (°)	θ (°)	$\mathbf{r}_{\mathrm{ECI}}$ (km)
Pass 1	0.069 746 1	58,603.6	51.9228	300.4945	144.7748	359.5405	-823, 7108, 3698
TLE 1	0.001 209 2	56,891.5	51.9974	67.7982	184.1231	1.8947	-2563, -7665, -670
TLE 2	0.000 543 3	56,489.2	52.0160	303.6990	319.9573	182.0047	-973, 6934, 3890
TLE 3	0.000 098 6	55,957.0	51.9981	329.5396	139.5293	86.7281	-6453, -259, -4472

The predicted inclination and angular momentum matched all three candidates well. The difference in eccentricity is relatively large but is still small on an absolute scale since the orbit is already very close to being circular. The argument of perigee and true anomaly are much more varied since all of the candidate objects are in near-circular orbits. It is readily apparent that the most likely candidate for the single pass observation is TLE 2 since the right ascension of ascending node and position vectors are closest to the prediction. The look angles for the observation and TLE 2 on 25 March 2013 at 3:15:20 UT are compared below:

Object	Azimuth (°)	Elevation (°)
Pass 1	240.8	35.6
TLE 2	244.0	40.2
Error	3.2	4.6

Unfortunately, the error would result in a missed observation if using a telescope with a field of view of 2.5°. Note that the epoch for TLE 2 is March 24, and the epoch for the other two TLEs are April 19 and April 14, so back-propagation of the TLE for days to weeks without accounting for perturbations introduces potential error.

2.2 Double Pass

The orbital elements corresponding to the calculated orbit and candidate TLEs for the double pass observations on 11 May 2013 at 3:46:48 UT and 5:47:30 UT are as follows:

Object	e	h (km s^{-2})	i (°)	Ω (°)	ω (°)	θ (°)	$\mathbf{r}_{\mathrm{ECI}}$ (km)
Pass 1	0.055 662 9	55,032.2	51.9120	30.0173	314.1999	177.1093	-6463, 571, 4756
TLE 4	0.000 191 1	56,786.9	51.996	32.8455	29.4868	124.7077	-7296, -2129, 2775
TLE 5	0.000 166 8	55,729.5	52.0023	49.6249	319.9573	116.9743	-2419, 4369, 5982
TLE 6	0.000 212 4	56,612.3	51.9963	156.5112	149.5293	72.3605	-3024, 4834, -4131
Pass 2	0.032 077 0	55,761.0	52.3711	29.6864	320.2769	171.4891	-6479, 530, 4759
TLE 4	0.000 191 1	56,786.9	51.996	32.8455	29.4868	124.7279	-7296, -2131, 2773
TLE 5	0.000 166 8	55,729.5	52.0023	49.6249	319.9573	137.8738	-4309, 2270, 6084
TLE 6	0.000 212 4	56,612.3	51.9963	156.5112	149.5293	85.3167	5859, 1867, -5180

Again, the predicted inclination and angular momentum matched all three candidates well. The same trend holds for RAAN, argument of perigee and true anomaly as in the single pass observations. However, this time it is much more difficult to discern the most likely candidate due to their inconsistent position vectors, so we must look at the difference in look angles instead. The look angles for the observations and TLEs on 11 May 2013 at 3:46:48 UT and 5:47:30 UT are compared below:

Object	Azimuth (°)	Elevation (°)
Pass 1	80.0	54.3
TLE 4	110.5	7.2
TLE 5	308.8	-1.0
TLE 6	214.0	-37.6
Pass 2	279.3	31.4
TLE 4	176.2	34.0
TLE 5	311.3	0.7
TLE 6	201.9	-87.2

It seems that TLE 4 is the most likely candidate simply by virtue of being the only candidate that is observable at one of the observation times. However, this is not a strong prediction as the elevation during pass 1 is likely too low to be observable and both azimuth and elevation are much different than the observation for this pass. Using a statistical orbit determination method with an integrated multi-rev solver may have yielded more accurate results than using extended Gauss twice on two subsets of the data.